Laboratory Investigation (2011) 91, 24–32

Pkd1-inactivation in vascular smooth muscle cells and adaptation to hypertension

Sabrine Hassane[1,5], Nanna Claij[1,5], Martine Jodar[2,5], Alexandra Dedman[2], Inger Lauritzen[2], Fabrice Duprat[2], Jorine S Koenderman[1], Annemieke van der Wal[3], Martijn H Breuning[1], Emile de Heer[3], Eric Honore[2], Marco C DeRuiter[4] and Dorien JM Peters[1]

Autosomal dominant polycystic kidney disease (ADPKD) is a multisystem disorder characterized by renal, hepatic and pancreatic cyst formation and cardiovascular complications. The condition is caused by mutations in the *PKD1* or *PKD2* gene. In mice with reduced expression of *Pkd1*, dissecting aneurysms with prominent media thickening have been seen. To study the effect of selective disruption of *Pkd1* in vascular smooth muscle cells (SMCs), we have generated mice in which a floxed part of the *Pkd1* gene was deleted by Cre under the control of the *SM22* promotor (*SM22-Pkd1*$^{del/del}$ mice). Cre activity was confirmed by X-gal staining using *lacZ* expressing Cre reporter mice (*R26R*), and quantitative PCR indicated that in the aorta *Pkd1* gene expression was strongly reduced, whereas *Pkd2* levels remained unaltered. Histopathological analysis revealed cyst formation in pancreas, liver and kidneys as the result of extravascular Cre activity in pancreatic ducts, bile ducts and in the glomerular Bowman's capsule. Remarkably, we did not find any spontaneous gross structural blood vessel abnormalities in mice with somatic *Pkd1* gene disruption in SMCs or simultaneous disruption of *Pkd1* in SMCs and endothelial cells (ECs). Extensive isometric myographic analysis of the aorta did not reveal differences in response to KCl, acetylcholine, phenylephrin or serotonin, except for a significant increase in contractility induced by phenylephrin on arteries from 40 weeks old *Pkd1*$^{del/+}$ germ-line mice. However, *SM22-Pkd1*$^{del/del}$ mice showed significantly reduced decrease in heart rate on angiotensin II-induced hypertension. The present findings further demonstrate *in vivo*, that adaptation to hypertension is altered in *SM22-Pkd1*$^{del/del}$ mice.
Laboratory Investigation (2011) **91,** 24–32; doi:10.1038/labinvest.2010.159; published online 20 September 2010

KEYWORDS: glomerular cysts; hypertension; *Pkd1*; polycystic kidney disease; SM22Cre; Tie2Cre

Autosomal dominant polycystic disease (ADPKD) is one of the most common inherited diseases, affecting 1:1000 individuals worldwide. The disease is characterized by progressive kidney enlargement and destruction of the normal renal tissue by many fluid-filled cysts, and progresses to end-stage renal failure (ESRF) in most patients. However, it is a slowly progressive disease with ESRF usually around the age of 60.[1] Approximately 85% of cases are because of *PKD1* mutations and in 15% the disease is caused by a mutation in *PKD2*.[2] Both *PKD1* and *PKD2* are expressed in a variety of cell types and tissues including renal epithelium, hepatic bile ducts, pancreatic ducts, vascular smooth muscle cells (SMCs) and endothelial cells (ECs).[3–5] ADPKD is also associated with cysts in the liver and pancreas as well as cardiovascular complications such as hypertension and aneurysms.[6]

High blood pressure is very common in ADPKD, and occurs in the majority of patients before any substantial reduction in renal function is observed. Furthermore, hypertension occurs at a much earlier age in patients with ADPKD than in the general population and is also associated with a rapid progression toward renal failure and increased cardiovascular complications (for review see ref. 7). The prevalence of cerebral aneurysms in ADPKD patients is approximately 10-fold higher than in the general population and about 27% among ADPKD patients with a family history for aneurysms.[8,9] Aneurysmal involvement of extracranial

[1]Center for Human and Clinical Genetics, Leiden University Medical Center, Leiden, The Netherlands; [2]Institut de Pharmacologie Moléculaire et Cellulaire, UMR CNRS 6097, Université de Nice Sophia Antipolis, Valbonne, France; [3]Department of Pathology, Leiden University Medical Center, Leiden, The Netherlands and [4]Department of Embryology and Anatomy, Leiden University Medical Center, Leiden, The Netherlands
Correspondence: Dr DJM Peters, Department of Human Genetics, Center for Human and Clinical Genetics, Leiden University Medical Center, Postal zone: S-04-P, P.O. Box 9600, 2300 RC, Leiden, The Netherlands.
E-mail: d.j.m.peters@lumc.nl
[5]These authors contributed equally to this work.

Received 21 April 2010; revised 20 June 2010; accepted 2 July 2010

arteries, such as the coronary arteries, abdominal aorta, renal artery and splenic artery has also been reported in patients with ADPKD (for review see ref. 7).

Several mouse models have been established to study ADPKD using targeted disruption of the *Pkd1* or *Pkd2* gene. Homozygous *Pkd1* and *Pkd2* knock-out mice die *in utero*, around embryonic day 15, because of severe cystic disease, vascular defects and/or abnormalities of the placental labyrinth, whereas heterozygous *Pkd1* knock-out mice showed minimal renal cyst formation in adulthood.[4,10–15] Furthermore, we described a *Pkd1* mouse (hypomorphic) model, with low expression of *Pkd1* showing progressive polycystic kidney disease and aortic dissecting aneurysms, indicating that *Pkd1* is implicated in the structural integrity and function of the vasculature.[16,17]

In the hypomorphic $Pkd1^{nl,nl}$ mice a very prominent media thickening was seen in most of the animals analyzed. As SMCs is the most abundant cell type in the media, we set out to study the effect of *Pkd1* gene disruption in vascular SMCs on blood vessel function. To this aim, we generated mutant mouse lines with a targeted disruption of the *Pkd1* gene in SMCs, by crossing mice containing floxed *Pkd1* alleles with *SM22Cre*. We previously showed that *Pkd1* gene disruption in vascular SMCs results in a reduced myogenic tone.[18]

Functional roles for the polycystins in mechanosensation have been proposed in ECs as well as SMCs. In ECs, the proteins are involved in fluid shear stress sensing, thereby regulating calcium signaling and nitric oxide release. This affects the vasodilatation in response to increased blood flow.[19] In vascular SMCs, the polycystins regulate the activity of the stretch-activated cation channels. In mice with reduced *Pkd1* expression in SMCs, stretch-activated channel (SAC) activity was decreased and the threshold pressure for myogenic contraction was significantly shifted to higher pressure values.[18] The ratio of polycystin-1/polycystin-2 regulates SACs activity, as polycystin-2 inhibits channel opening, whereas polycystin-1 reverses this inhibition.[18]

It is likely that alterations in intracellular Ca^{2+} homeostasis contribute to the vascular phenotype in PKD.[20,21]

In this study, we show that disruption of the *Pkd1* gene in these cells did not induce gross structural abnormalities in blood vessels, even not when *Pkd1* was disrupted in ECs, as well. However, an increase in blood pressure in $SM22\text{-}Pkd1^{del/del}$ mice, induced by angiontensin II treatment, resulted in reduced heart rate adaptation.

MATERIALS AND METHODS

Mice

The generation of $Pkd1^{del2\text{-}11}$ and $Pkd1^{lox2\text{-}11}$ alleles has been described previously.[17,22] The $Pkd1^{lox2\text{-}11}$ ($Pkd1^{lox}$) allele contains two *loxP* sites inserted into intron 1 and 11. In the presence of the DNA recombinase Cre, the *loxP* flanked sequence was deleted to form the $Pkd1^{del2\text{-}11}$ ($Pkd1^{del}$) allele. The floxed *Pkd1* mice were crossed with *SM22Cre* mice (Tgln-Cre, Jackson laboratories, Bar Harbor, USA) to target SMC or with *Tie2Cre* mice (kindly provided by Dr B Arnold, Heidelberg, Germany) to target ECs. This yielded $SM22Cre^{+}\text{-}Pkd1^{del/del}$ mice ($SM22\text{-}Pkd1^{del/del}$) and $Tie2Cre^{+}\text{-}Pkd1^{del/del}$ mice ($Tie2\text{-}Pkd1^{del/del}$). To generate $SM22Cre^{+};Tie2Cre^{+}\text{-}Pkd1^{del/del}$ mice ($SM22;Tie2\text{-}Pkd1^{del/del}$), $SM22\text{-}Pkd1^{del/del}$ mice were crossed with $Tie2\text{-}Pkd1^{del/del}$ mice. Littermates that were homozygous or heterozygous for the floxed *Pkd1* gene and mice only expressing the Cre transgene, were used as controls. To analyze Cre activity *in vivo*, *Tie2Cre* and *SM22Cre* mice were crossed with the *ROSA26 (R26R) LacZ*-expressing Cre reporter mice.[23]

All experiments using mice were approved according to the Dutch and French law and conform with the Guide for the Care and Use of Laboratory Animals published by the US National Institutes of Health (NIH publication no. 85-23, revised 1996). Approval was granted by a local ethics review board.

PCR for *Pkd1* Gene Disruption in ECs and Vascular SMCs

Genotypes were assessed by PCR analysis of tail genomic DNA using a reverse primer in intron 11 combined with a forward primer in intron 1 (del allele) or a forward primer in intron 11 (floxed and wild-type alleles) as described previously for genotyping of strains.[22]

Real-Time Quantitative PCR

Quantitative PCR was performed on mRNA isolated from aortas of 30-week-old $SM22\text{-}Pkd1^{del/del}$, $SM22\text{-}Pkd1^{+/del}$ and control mice. For quantitative PCR (qPCR) analysis, primer sequences are as follow: *Pkd1*: forward: GCC ATC CAG CAC TTC CTA GT, reverse: GAG AAG CCG ATC CAC ACA TC; *Pkd2*: forward: AGGTGTTAGGACGGCTGCT, reverse: CCCTGTGGATCTCACTGTCC. qPCR data were normalized to the mouse *Top1* reference gene expression amplified using the following primers: *Top1:* forward: GCCTCCATCACACTACAGCA and reverse: TTCGCTGGT ACATTCTCATCA. qPCR data were analyzed using the LightCycler 480 software release 1.5.0 and Excel program, as described previously.[18]

Immunohistochemistry

Histological analysis was performed on aortas (from aortic root to the bifurcation of the iliac arteries), pancreas, liver and kidneys. The organs were dissected and fixed in 4% paraformaldehyde in 0.1 M sodium phosphate buffer for 24 h. Fixed tissues were dehydrated in graded ethanol and xylene and embedded in paraffin. Sequential sections of 4 μm were mounted onto Superfrost-plus glass slides. After deparaffinization, sections were stained using standard procedures.[24] Sections were incubated in 0.1 mg/ml pronase before incubation with CD31 (PECAM) and Lyve-1 antibodies. The monoclonal 1A4 antibody (α-SM-actin) and secondary antibody rabbit–anti-mouse peroxidase (RAM-PO) were first incubated to form 1A4-RAM-PO complex before adding it on sections following a previously described procedure.[25] The

antibody complexes were visualized using 0.04% diaminobenzidine-tetra-hydrochloride. The following histochemical stainings were preformed; hematoxylin eosin and resorcin fuchsin for elastin lamellae.

Antibodies

The following primary antibodies were used: CD31 (1:50, BD Bioscience, Erembodegem, Belgium), Lyve-1 (1:1000, Reliatech, Wolfenbüttel, Germany), α-smooth muscle actin (1A4, 1:2000, Sigma-Aldrich, Zwijndrecht, The Netherlands), anti-megalin (1:500, Pathology, Leiden, The Netherlands),[26] anti-Tamm Horsfall (uromodulin; 1:3000, CAPEL, Durham, NC, USA), anti-aquaporin-2 (1:300, Calbiochem, Amsterdam, The Netherlands).

Secondary antibodies were: rabbit envision/horseradish peroxidase (HRP; undiluted; Dako, Heverlee, Belgium) and rabbit-anti-goat Ig/HRP (1:100, Dako, Heverlee, Belgium), goat anti-rat-biotin (1:200, BD Bioscience), goat serum (1:100, Brunschwig chemie, Amsterdam, The Netherlands), mouse biotinylated (ABC-kit vectastain; 1:100, Brunschwig Chemie, Amsterdam, The Netherlands).

X-Gal Staining

Tissues of 3-day-old *SM22Cre*; *R26R* and *Tie2Cre;R26R* mice and controls were stained whole mount for X-gal (see Supplementary Methods). After washing tissues were post-fixed overnight in phosphate-buffered 4% formaldehyde and further processed for embedding in paraffin. Sections of 4 μm were cut and counter stained with 0.1% nuclear fast red and 5% $Al_2(SO_4)_3$ for 5–10 s.

Tail Cuff Measurements and Osmotic Pumps Implantation

Systolic blood pressure and heart rate were measured by the tail cuff method (BP2000, Visitech), at 37°C to dilate the tail artery, five times weekly and averaged for each week. *SM22-Pkd1*$^{del/del}$ and control wild-type mice (50% *Pkd1*$^{lox/lox}$ and 50% *SM22Cre*), 30 weeks old, were habituated to the measurement for 3 weeks before implantation of the pumps and then monitored during about 4 weeks. The osmotic pumps (Alzet model, 2004) were implanted subcutaneously on the back of the animals and continuously delivered a dose of 0.61 mg per kg per day of angiotensin II (AngII; Sigma) in phosphate buffer saline. Systolic blood pressure and heart rate were recorded simultaneously. Significance of the two groups was tested with a permutation test (non-parametric test) at a threshold of 5%; StatXact software).

To study the effects of elevated blood pressure on vessel structure, the thoracic aortas of control (*Pkd1*$^{lox/lox}$ and *SM22Cre*) and *SM22-Pkd1*$^{del/del}$ mice were observed. Fixation was carried out by perfusion with Bouin's fixative (formalin/picric acid) in the animal during 10 min and after removal from the animal in 10% neutral-buffered formalin. Tissues were paraffin-embedded, sectioned, and stained with combined orcein (dark elastin staining) and picro-indigo-carmin (blue collagen staining).

Wire Myography

A 2 mm long segments of thoracic aorta were mounted on a wire myograph (DMT, Aarhus, Denmark; isometric myography).[27] Two steel wires (40 μm in diameter) were inserted into the artery lumen and fixed to a force transducer and a micrometer, respectively. A normalization procedure was used to evaluate the internal circumference that the aorta would have under a transmural pressure of 100 mm Hg (IC 100). To obtain a maximal and uniform response, all experiments were carried out at 90% of this internal circumference (IC 90). Arteries were bathed in a physiological solution (PSS), which composed of (in mM) NaCl 119; KCl 4.7; $CaCl_2$ 2.5; $MgSO_4$ 1.17; $NaHCO_3$ 25; KH_2PO_4 1.18; EDTA 0.027; glucose 5.5, oxygenated with a mixture of CO_2 (5%) and O_2 (95%), or the same PSS solution containing 80 mM KCl (NaCl substituted by KCl), named PSS 80K. Before each experiment, the contractility of the muscle was tested using the PSS 80K solution and then phenylephrin (1 μM) in standard PSS. The integrity of the endothelium was assessed by verifying that at least a 70% relaxation effect was obtained with acetylcholine (5 μM) after a precontraction by phenylephrin (1 μM). For each mouse, between two to four responding aorta rings were measured and averaged, error bars indicates the standard error to the mean, *n* indicates the number of mice. Significance was tested with a permutation test (R; R Development Core Team: http://www.r-project.org/) at a threshold of 5% (*), 1% (**) and 1‰ (***). Cumulative dose response curves of phenylephrin, serotonin (5HT) and U46619 (thromboxan A2 agonist) were realized with extensive washout in between each curve. The cumulative dose response curve of acetylcholine was made after a precontraction with phenylephrin (1 μM). Experiments were performed on heterozygous *SM22-Pkd1*$^{del/+}$ mice and controls (*SM22Cre* and *Pkd1*$^{lox/+}$), homozygous *SM22-Pkd1*$^{del/del}$ mice and their controls (*SM22Cre* and *Pkd1*$^{lox/lox}$) at 11 weeks, as well as heterozygous *SM22-Pkd1*$^{del/+}$ mice and their controls and the germ-line *Pkd1*$^{del/+}$ and wild types, on mice aged 40 weeks.

RESULTS

Inactivation of Pkd1 in Smooth Muscle and ECs Does Not Result in Gross Structural Blood Vessel Abnormalities

To inactivate *Pkd1* in SMCs, we crossed *Pkd1*$^{del/lox}$ and *Pkd1*$^{del/lox}$ mice with *SM22Cre* mice to yield *SM22-Pkd1*$^{del/del}$. We carefully analyzed aortas of six *SM22-Pkd1*$^{del/del}$ mice (age 6 months) with *Pkd1* gene disruption in SMCs but did not see any abnormalities. As the matrix metalloproteinase (MMP)-2 and -9, are key activators in blood vessel remodeling we performed zymography to analyze MMP-2 and MMP-9 activity. No differences were observed between the different genotypes (not shown). Subsequently, we inactivated *Pkd1* in both SMCs and ECs by crossing

SM22-Pkd1$^{del/del}$ with *Tie2-Pkd1*$^{del/del}$ mice to yield SM22;*Tie2-Pkd1*$^{del/del}$ mice. We carefully analyzed aortas of four *SM22;Tie2-Pkd1*$^{del/del}$ mice (age 6 months). Also these aortas were morphologically normal (Figure 1a–c). As combined inactivation of *Pkd1* in SMCs and ECs did not show any vascular phenotype, we did not further analyze the aortas of *Tie2-Pkd1*$^{del/del}$ mice with Cre activity only in ECs.

Inactivation of Pkd1 in SM22Cre Expressing Cells Induces Cysts in Pancreas, Liver and Kidneys

All neonatal *SM22-Pkd1*$^{del/del}$ mice (age 3 and 4 days, $n=7$) showed a few large and small pancreatic cysts (Figure 1f) as well as dilated glomeruli in kidneys. The liver showed no cysts at this age. Most mice survived and were killed at the age of 6 months, ($n=10$) large cysts were found in pancreas, liver and kidneys (Figure 1g–i).

Cysts in pancreas and liver were surrounded by spindle-like cells, which were positive for α-smooth muscle actin (α-SMA, not shown) indicating infiltration of myofibroblasts (Figure 1, insets in g and h). The cysts were localized in groups, and few cysts were hyperplastic. In the pancreas, the cystic phenotype was more progressive compared with kidneys and liver, with larger numbers and sizes of cysts. Cysts in the pancreas and liver seem to originate from the pancreatic ducts and bile ducts, respectively, whereas no loss of pancreatic acini or hepatocytes in liver were detected.

In the kidneys, a few dilated glomeruli, one to six dilatations per section, were found in neonates at day 3. In 6-month-old mice, large cysts were found and many of these cysts contained the glomerular tuft, which stained for the endothelial marker CD31, indicating the presence of glomerulus-derived cysts (Figure 1i). Not all glomeruli were dilated and kidneys showed many normal glomeruli as well.

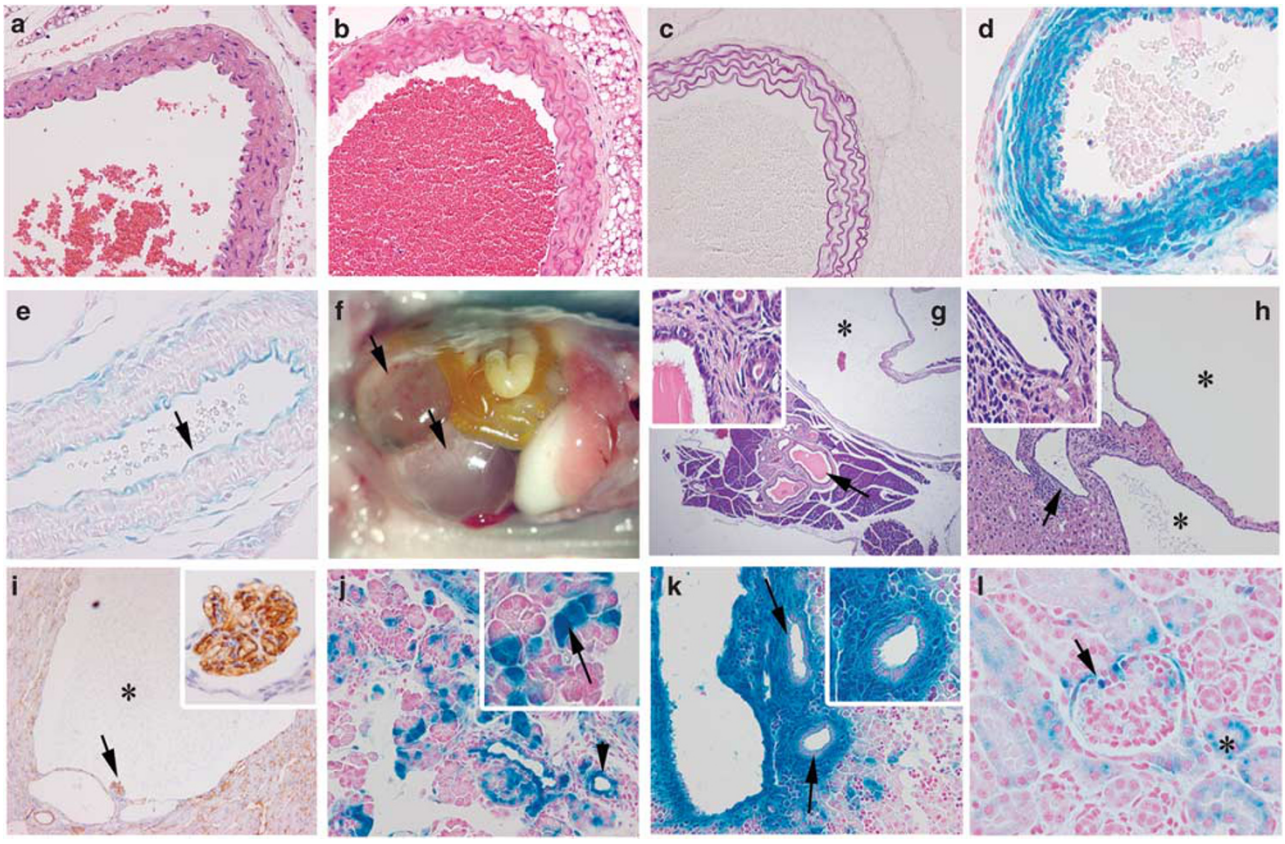

Figure 1 Blood vessel structure and cyst formation in *SM22-Pkd1*$^{del/del}$ mice; the activity of Cre in *SM22Cre* and *Tie2Cre* mice. (**a**) Wild-type aorta, hematoxylin eosin staining. (**b**) *SM22-Pkd1*$^{del/del}$ aorta, hematoxylin eosin staining. (**c**) *SM22-Pkd1*$^{del/del}$ aorta, elastin lammelae staining. (**d**) Cre-induced *LacZ* activity in smooth muscle cells in aorta of 3-day-old *SM22Cre;R26R* mouse. (blue staining) (**e**) *Tie2Cre*-induced *LacZ* activity in endothelial cells (arrow) in the aorta of 3-day-old *Tie2Cre;R26R* mouse (blue staining). (**f–i**) Organs of *SM22-Pkd1*$^{del/del}$ mice. (**f**) Large pancreatic cysts (arrows) in the abdomen of 3-day-old *SM22-Pkd1*$^{del/del}$ mouse. (**g**) Small pancreatic cysts (arrow) and large cysts (asterisk). (**h**) Small (arrow) and large cysts (asterisk) in liver. Insets in **g** and **h** show fibrotic tissue around cysts. (**i**) Glomerular cysts (asterisk). Inset shows CD31 staining in glomerulus. (**j–l**) Recombination of *lacZ* (blue staining) under control of *SM22* promotor in different organs of 3-day-old *SM22Cre;R26R* mice. (**j**) *lacZ* expression in pancreatic ducts (arrowhead). Inset show some acini cells express *lacZ* (arrow). (**k**) *SM22Cre* activity in liver. Bile ducts express *lacZ* (arrow and inset). (**l**) *SM22Cre* activity in kidney. The parietal layer of Bowman's capsule of mature glomeruli express *lacZ* (arrow). Cortical tubules show non-specific staining (asterisk), which is also observed in control *R26R* mice (not shown).

None of the cysts stained positive for the nephron segment-specific markers (megalin for proximal tubules, Tam Horsfall protein for distal tubules and loops of Henle and aquaporin-2 for collecting ducts). We also did not find dilatations of lymphatic or blood vessels, as determined by Lyve-1, CD31 and α-SMA staining.

Tie2-Pkd1$^{del/del}$ mice ($n=13$) did not show any abnormalities in the liver, kidneys and pancreas at the age of 7, 8, 10 and 12 months. Only two mice showed one cyst in the liver (age 7 and 10 months). The *SM22;Tie2-Pkd1*$^{del/del}$ mice with Cre activity in both SMCs and ECs ($n=7$) showed the same phenotype as the *SM22-Pkd1*$^{del/del}$ mice. Taken together, these results indicate that the *Tie2-Pkd1*$^{del/del}$ genotype does not cause gross structural abnormalities, whereas the *SM22-Pkd1*$^{del/del}$ genotype is responsible for the cysts formation in the different organs of the *SM22-Pkd1*$^{del/del}$ and *SM22;Tie2-Pkd1*$^{del/del}$ mice.

Cre Activity in Aortas of SM22Cre and Tie2Cre Mice

To monitor the activity of Cre in the *SM22Cre*$^{+}$ and *Tie2Cre*$^{+}$ mice, we crossed these mice with a *LacZ* expressing Cre reporter mouse line, *R26R*.[23] X-gal staining of *SM22Cre*;*R26R* (age 3 days, $n=2$) aortas, revealed that efficient recombination of the reporter construct had occurred in SMCs in the media and the adventitia, resulting in expression of the *LacZ* gene (Figure 1d). In *Tie2Cre*;*R26R* (age 3 days, $n=1$), *LacZ* expression was found in most ECs in the intima (Figure 1e).

Pkd1 gene disruption by Cre was confirmed by PCR analysis of the DNA derived from the tails of mice carrying the *Pkd1*$^{lox/+}$ alleles as well as *SM22Cre* or *Tie2Cre* (Figure 2a). Even more, quantitative PCR revealed a strong reduction in *Pkd1* mRNA levels in aorta's of *SM22-Pkd1*$^{del/del}$ mice compared with *SM22-Pkd1*$^{del/+}$ and controls, whereas *Pkd2* mRNA levels remained unaltered (Figure 2b).

Cre Activity in Pancreas, Liver and Kidneys of SM22Cre and Tie2Cre Mice

To explain the phenotype of the *SM22-Pkd1*$^{del/del}$ mice, we analyzed Cre activity in the kidneys, liver and pancreas in *SM22Cre*;*R26R* mice (age 3 days). X-gal staining was found in all three organs and it matched with the origin of cyst formation found in these organs in *SM22-Pkd1*$^{del/del}$ mice. In the pancreas, many serous acini and the ducts were positive for *lacZ* expression (Figure 1j). In the liver, expression was found in most bile ducts and in mesenchymal cells around the ducts (Figure 1k). In addition, blood cell precursors, eg, myeloblasts, myelocytes, granulocytes and megakaryocytes were also positive for *lacZ*. Hepatocytes did not show *lacZ* expression. The kidneys showed *lacZ* expression in the parietal layer of Bowman's capsule of mature glomeruli (Figure 1l). The control *R26R* mice, without the Cre transgene, did not show X-gal staining, except for a subset of proximal tubules. This was also found in the renal cortical tubules of *SM22Cre*;*R26R* and *Tie2Cre*;*R26R*, indicating non-specific signal (Figure 1l). SMCs of blood vessels in all organs were positive for X-gal.

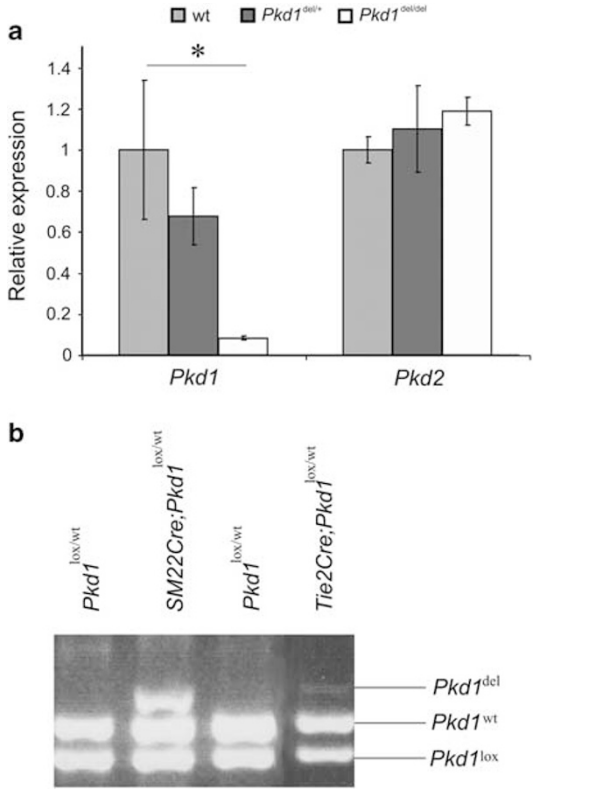

Figure 2 *SM22Cre* and *Tie2Cre*-mediated recombination of the floxed *Pkd1* allele. (**a**) *Pkd1* and *Pkd2* mRNA levels in aorta's from *SM22-Pkd1*$^{del/del}$ ($n=13$), *SM22-Pkd1*$^{del/+}$ ($n=9$) or control ($n=31$) mice. Expression was normalized to the housekeeping gene. Results are presented as mean ± s.d. of expression relative to the expression of controls. (**b**) Agarose gel analysis of PCR products amplified from genomic DNA isolated from tails of adult *SM22-Pkd1*$^{lox/wt}$, *Tie2-Pkd1*$^{lox/wt}$ and *Pkd1*$^{lox/wt}$. Three bands can be seen for both *Tie2-Pkd1*$^{lox/wt}$ and *SM22-Pkd1*$^{lox/wt}$ mice; the wild-type (wt) *Pkd1* allele (*Pkd1*^{wt}), the floxed *Pkd1* allele (*Pkd1*^{lox}) and the partially deleted *Pkd1* (*Pkd1*^{del}) indicating that floxed *Pkd1* allele is deleted on Cre expression in both mouse models. The intensity of the 366-bp deletion-specific PCR product is relatively weak compared with the floxed or wt alleles, as Cre-mediated recombination occurred only in smooth muscle cells or endothelial cell, respectively. In control mice, without Cre, the deletion-specific product was absent. *$P<0.05$.

Deletion of *Pkd1* under the control of *Tie2* promotor did not result in a phenotype. *Tie2Cre*;*R26R* reporter mice, neonatal age 3 days, showed *lacZ* expression in ECs in large vessels (Figure 1e), in capillaries, and in blood cell precursors (not shown), which is in line with previous reports.[28]

Selective Inactivation of Pkd1 in SMCs does not Affect Contractility

To analyze whether *Pkd1* gene deletion has more subtle effects on vascular function, several series of isometric myographic analyses were performed on aortas. First, heterozygous *SM22-Pkd1*$^{del/+}$ mice and controls as well as homozygous *SM22-Pkd1*$^{del/del}$ mice and their controls were analyzed at 11 weeks

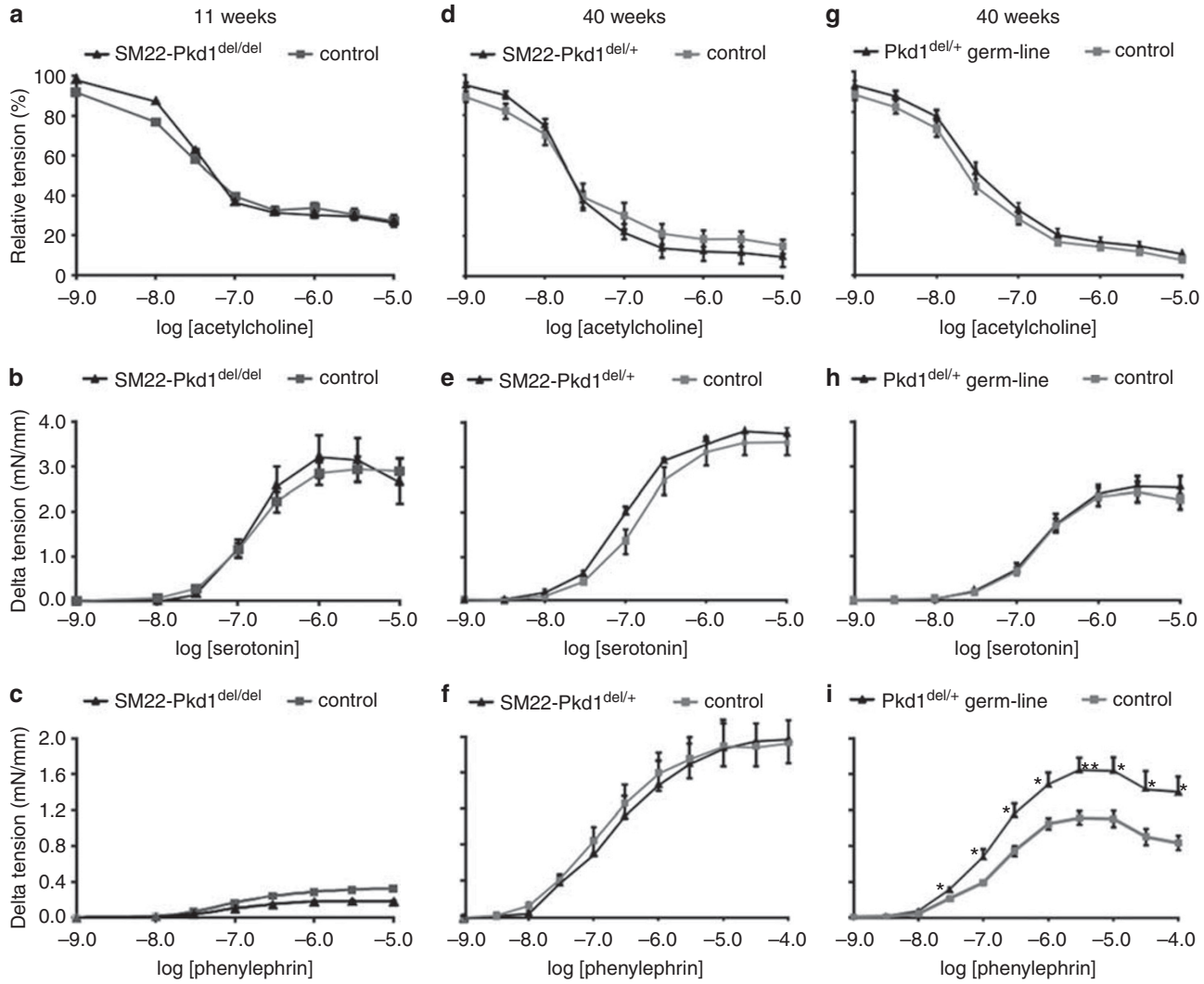

Figure 3 Myographic analysis on aorta from 11–week- and 40-week-old mice. (**a, d, g**) Dose–effect curve of the variation in tension, relative to precontracted tension, induced by different concentrations of acetylcholine. Doses were added cumulatively after a precontraction with 1 μm phenylephrin. Experiments were carried out on 11-week-old mice *SM22-Pkd1*$^{del/del}$ ($n=22$) and their controls (*SM22Cre* and *Pkd1*$^{lox/lox}$, $n=55$) (**a**), and on 40-week-old *SM22-Pkd1*$^{del/+}$ ($n=10$) and their controls (*SM22Cre* and *Pkd1*$^{lox/+}$, $n=16$) (**d**), as well as with *Pkd1*$^{del/+}$ germ-line mice ($n=17$) and their controls (wild type, $n=12$) (**g**). (**b, e, h**) Dose–effect curve of the variation in tension, relatively to resting tension, induced by various concentrations of serotonin. Doses were added cumulatively and experiments were carried out on the same mice as in **a**, **d** and **g**. (**c, f, i**) Dose–effect curve of the variation in tension, relatively to resting tension, induced by various concentrations of phenylephrin. Doses were added cumulatively and experiments were carried out on the same mice as in **a, d, g**.

of age (Figures 3a–c). At this age the IC 90 (internal diameter at 90 mm Hg pressure) is small, around 415 μm, and vasoconstriction induced by phenylephrin is low (0.2 mN/mm at 10^{-5} M; Figure 3c). No differences were observed between the different genotypes (Figure 3c). We also found no differences between IC 90 at vasoconstriction obtained with passive depolarization of the vessels with 80 mM KCl (PSS 80 K), between activation curves obtained with serotonin or the vasoconstrictor U46619, and when looking at dilatation obtained with acetylcholine (Figures 3a and b).

Next series of measurements were performed on the heterozygous *SM22-Pkd1*$^{del/+}$ mice and their controls, as well as the germ line *Pkd1*$^{del/+}$ (which carry a deletion allele in all cells) and wild-type controls, both performed on older mice, aged 40 weeks (Figures 3d–i). The homozygous mutants *SM22-Pkd1*$^{del/del}$ were not available because of the cystic phenotype (see above). No differences were found between the IC 90, with 1029 ± 16 μm and 1053 ± 9 μm for *SM22-Pkd1*$^{del/+}$ ($n=10$) and their controls ($n=16$), respectively, ($P=0.49$), and with 967 ± 10 μm and 979 ± 10 μm for *Pkd1*$^{del/+}$ ($n=17$) and their control wild types ($n=12$), respectively, ($P=0.79$). The vasodilatation induced by acetylcholine was not significantly different in both series of experiments (Figures 3d and g). The vasoconstriction induced by

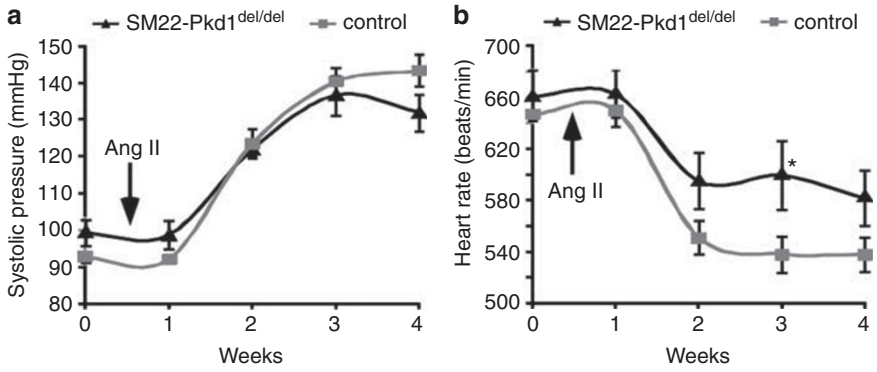

Figure 4 (**a**) Systolic blood pressure and (**b**) heart rate measured in *SM22-Pkd1*$^{del/del}$ ($n=6$) and their controls (*SM22Cre* mice and *Pkd1*$^{lox/lox}$ littermates, $n=18$) at 1 to 4 weeks of angiotensin II (AngII) infusion. Mean ± s.e.m. are shown. Difference in heart rate is significant at week 3 ($P=0.041$). The five measurements during each week were averaged. The pumps containing AngII were implanted between week 0 and week 1.

depolarization with 80 mM KCl was not different in both series (not shown). No difference was observed neither on the vasoconstriction induced by serotonin (Figures 3e and h), nor on the one obtained with U46619 (not shown). The vasoconstriction induced by phenylephrin was not different between smooth muscle-specific heterozygous *SM22-Pkd1*$^{del/+}$ and their controls (Figure 3f). Interestingly, they were significantly higher in the germ-line *Pkd1*$^{del/+}$ mice compared with wild type ($P=0.007$ at 3 μM), as previously reported by Morel *et al* (2009) for 30-week-old mice (Figure 3i).[20]

Increased Blood Pressure Induces Mild Media Thickening and Impaired Adjustment of Heart Rate in SM22-Pkd1$^{del/del}$ Mice

As the hypomorphic *Pkd1*$^{nl/nl}$ mice show a strong renal cystic phenotype, it is anticipated that those mice have an elevated blood pressure, which could contribute to the vascular pathology. As baseline arterial pressure was not altered in *SM22-Pkd1*$^{del/del}$ mice compared with controls.[18] We induced high blood pressure by the infusion of AngII (Figure 4). Histological analysis induced mild media thickening but did not reveal gross structural differences between Angiotensin II treated *SM22-Pkd1*$^{del/del}$ mice and controls (not shown).

Interestingly, AngII induced decrease in the heart rate was significantly less pronounced in *SM22-Pkd1*$^{del/del}$ ($P=0.041$, at 3 weeks), although the systolic pressure response was not different (Figures 4a and b).

DISCUSSION

Previously, we analyzed a *Pkd1* hypomorphic mouse model, *Pkd1*$^{nl/nl}$, with reduced levels of *Pkd1* transcripts in the aortas and kidneys.[16] These mice showed dissecting aneurysm formation with very prominent abnormalities in the media and mild intima involvement. In addition, they have severe polycystic kidney disease.

In this study, we generated mouse models to analyze the consequences of the specific deletion of *Pkd1* in SMCs, which are the major component of the media. These mice, however, did not show any structural alterations of the aortic vessel wall in mice analyzed up to 6 months. Moreover, disruption of *Pkd1* simultaneously in SMCs and ECs did not result in structural blood vessel alterations, even though the recombination levels were high in blood vessels as shown by the Cre reporter and by strongly reduced *Pkd1* mRNA levels. This is in agreement with the early expression of endogenous *SM22* and *Tie2* genes, around embryonic day 8.[29,30] Our data indicate that *Pkd1* gene disruption in SMCs alone and/or in ECs is not sufficient to induce gross structural abnormalities in the aorta, suggesting that additional triggers are needed to induce or to accelerate the phenotype. For the renal cystic phenotype, we previously showed that the renal injury is a trigger that strongly accelerates the polycystic kidney disease.[31]

Extensive isometric myographic analysis did also reveal that no difference in response to KCl, acetylcholine, phenylephrin, U46619 or serotonin was observed in young mice (11 weeks) or in older mice (40 weeks), in heterozygous or in homozygous animals with a selective disruption of *Pkd1* in SMCs. Only the 40-week-old heterozygous *Pkd1*$^{del/+}$ mice, which carry a deletion allele in all cells, show a significant increase in vascular contractility in response to phenylephrin. This increase has been previously reported in the same mutants aged 30 weeks, whereas at 12 and 20 weeks no differences were observed.[17] Our results suggest that heterozygous *Pkd1* gene disruption in vascular SMCs is not sufficient to explain the increased phenylephrin response in *Pkd1*$^{del/+}$ mice and that other cell types probably contribute to this vascular phenotype. In addition, the effect is building up over time.

Importantly, although we did not observe spontaneous structural alterations in the aorta's of *SM22-Pkd1*$^{del/del}$ mice, these mice showed a decreased myogenic tone in resistance arteries.[18] Interestingly, the ratio of polycystin-1/polycystin-2, which is disturbed in the deletion mutants, is of crucial importance for the regulation of stretch-activated ion channels (SACs) in arterial myocytes.[18] Activation of SACs

regulates myocyte contraction and thereby the vascular tone. When we implanted the AngII-releasing pumps to induce hypertension, the heart rate significantly slowed down in all genotypes.

This decrease in heart rate is the result of adaptation of the cardiac outflow to increased peripheral resistance and/or to the central nervous system effect of angiotensin.[32,33] Interestingly, in the homozygous *SM22-Pkd1*$^{del/del}$ mice, this decrease in heart rate is significantly less prominent compared to the control mice. Cardiac output (stroke volume × heart rate) is known to drop upon an increase in blood pressure, as for instance induced by AngII infusion.[34] However, according to the classical Guyton model (Guyton *et al*, 1972), without autoregulation (ie, myogenic tone), cardiac output in response to hypertension is predicted to remain high.[32,34] This model fits nicely with our data as anticipated by a loss of myogenic tone in *SM22-Pkd1*$^{del/del}$ mice.[18] Indeed, in these mice, the decrease in heart rate (ie, cardiac output) is significantly less prominent compared with the control mice. Another possible mechanism of the hypertension-induced bradycardia may include a central effect through AT1 receptors in the central nervous system.[33]

Several other explanations could be given why without additional triggers the hypomorphic *Pkd1*$^{nl/nl}$ mice, and also *Pkd1* knock-out mice, show structural abnormalities of the blood vessels at neonatal or embryonic stages, respectively, while the *SM22;Tie2-Pkd1*$^{del/del}$ mice do not.[4,10,11,16] The genetic background may affect the process of blood vessel remodeling, as the complex mouse models used in this study consisted of a mixture of different genetic backgrounds. Furthermore, low *Pkd1* expression in other cell types than SMCs and Ecs, in which *Pkd1* is not disrupted in the *SM22;Tie2-Pkd1*$^{del/del}$ mice (for instance immune cells), may contribute to the process of aneurysm formation in *Pkd1*$^{nl/nl}$ mice, thereby accelerating the process. Therefore, it will be interesting to study the effects of increased blood pressure in *SM22;Tie2-Pkd1*$^{del/del}$ mice on full C57BL/6 background in future experiments.

Although no spontaneous structural abnormalities of the vasculature were detected, we observed cyst formation in pancreas, liver and kidneys, when the *Pkd1* gene was deleted under the control of *SM22* promotor. Expression of *LacZ* matched with the sites of cyst formation and was found in pancreatic ducts and hepatic bile ducts, which are the origin of the cysts. In the kidneys, only glomerular cysts were found and recombination did occur in the parietal layer of Bowman's capsule of glomeruli. It is known that *Pkd1* is also expressed in pancreatic ducts, hepatic bile ducts and Bowman's capsule, and thus coincides with the origin of the cysts as well.[5,35,36] These cysts can be found in ADPKD patients as well. Our data indicate that the SM22 promoter fragment that regulates the expression of Cre is not exclusively expressed in vascular SMCs. Expression of the promoter in specific mesenchymal cells during the development may explain the observed expression pattern.[37]

Despite the presence of large cysts, the function of the pancreas was not severely affected, as no loss of acini was found and there was no starch present in the colon, indicating a sufficient level of digestion (not shown). In the liver, no loss of hepatocytes was noticed either. Furthermore, the mutant kidneys showed many normal glomeruli beside the dilated ones. These results may explain why the mutant mice were able to survive for several months even with the presence of large cysts, especially in the pancreas.

The renal glomerular cystic phenotype was relatively mild and did not affect the blood pressure. Glomerular cysts can also be found as part of ADPKD, predominantly in fetal kidneys and also in adult end-stage kidneys, in addition to tubular cysts.[38,39] In addition, glomerular cysts can develop as distinct entity, glomerulocystic kidney disease or in the context of several other renal diseases.[40–42] Also in *Pkd1*-mutant mouse models glomerular cysts have been observed. These cysts were only observed in *Pkd1* knock-out mice but not in hypomorphic mice that have low levels of *Pkd1* gene expression, suggesting that total absence of *Pkd1* is necessary to induce the formation of glomerular cysts.[10,11,15,17,43,44] How these cysts arise is not entirely clear. As *Pkd1* is deleted in Bowman's capsule, the suggested mechanism that urinary tract infections lead to increased pressure in Bowman's space seems not very likely in *SM22-Pkd1*$^{del/del}$ mice.[45] Defects in cilia signaling, cellular signaling, cell–cell and cell–matrix interactions, which have been observed in ADPKD tubular cysts, probably have a more important role. In addition, as polycystin-1 is known to affect migration and proliferation,[46,47] the absence of *Pkd1* might disturb the recruitment of podocytes from the glomerular parietal epithelial cells, which proliferate and migrate into the glomerular tuft and differentiate into podocytes.[48]

In conclusion, targeted deletion of *Pkd1* in SMCs does not induce major structural blood vessel abnormalities, spontaneously, in mice. Increased blood pressure, however, revealed a mildly reduced adaptation of the heart rate. It remains to be determined whether the decrease in myogenic tone observed in these mice is involved in this phenotype.[18]

Supplementary Information accompanies the paper on the Laboratory Investigation website (http://www.laboratoryinvestigation.org)

ACKNOWLEDGEMENTS

The authors thank M van der Valk, DCF Salvatori, R Sandford (Cardiff), WN Leonhard, IS Lantinga-van Leeuwen, B Wisse and JC van Munsteren for support and discussion. We thank Dr B Arnold (Heidelberg) for the Tie2Cre mice. This work was supported by grants from the Dutch Heart Foundation (NHS, 2002B177), The Netherlands Organization for Scientific Research (NWO, VIDI 016.036.353) and the Leiden University Medical Center. We are grateful to the ANR 2005 cardiovasculaire-obésité-diabète, the ANR 2008 du gène à la physiopathologie, the Association for information and research on genetic kidney disease France, the Fondation del Duca, the Fondation de la recherche médicale, the Fondation de France, the Fondation de recherche sur l'hypertension artérielle, the Fédération pour la recherche sur le cerveau, the Société Générale AM, the Université de Nice Sophia Antipolis and the CNRS for financial support.

DISCLOSURE/CONFLICT OF INTEREST

The authors declare no conflict of interest.

1. Hateboer N, Dijk MA, Coto E, *et al.* Comparison of phenotypes of polycystic kidney disease types 1 and 2. Lancet 1999;353:103–107.
2. Peters DJM, Sandkuijl LA. Genetic heterogeneity of polycystic kidney disease in Europe. In: Breuning MH, Devoto M, Romeo G (eds). Contributions to Nephrology, Vol. 97: Polycystic Kidney Disease. Karger: Basel, 1992, pp 128–139.
3. Griffin MD, Torres VE, Grande JP, *et al.* Vascular expression of polycystin. J Am Soc Nephrol 1997;8:616–626.
4. Boulter C, Mulroy S, Webb S, *et al.* Cardiovascular, skeletal, and renal defects in mice with a targeted disruption of the Pkd1 gene. Proc Natl Acad Sci USA 2001;98:12174–12179.
5. Peters DJM, van der Wal A, Spruit L, *et al.* Cellular localization and tissue distribution of polycystin-1. J Pathol 1999;188:439–446.
6. Gabow PA. Autosomal dominant polycystic kidney disease. N Engl J Med 1993;329:332–342.
7. Ecder T, Schrier RW. Cardiovascular abnormalities in autosomal-dominant polycystic kidney disease. Nat Rev Nephrol 2009;5:221–228.
8. Chapman AB, Rubinstein D, Hughes R, *et al.* Intracranial aneurysms in autosomal dominant polycystic kidney disease. N Engl J Med 1992;327:916–920.
9. Ruggieri PM, Poulos N, Masaryk TJ, *et al.* Occult intracranial aneurysms in polycystic kidney disease: screening with MR angiography. Radiology 1994;191:33–39.
10. Kim K, Drummond I, Ibraghimov-Beskrovnaya O, *et al.* Polycystin 1 is required for the structural integrity of blood vessels. Proc Natl Acad Sci USA 2000;97:1731–1736.
11. Muto S, Aiba A, Saito Y, *et al.* Pioglitazone improves the phenotype and molecular defects of a targeted Pkd1 mutant. Hum Mol Genet 2002;11:1731–1742.
12. Pennekamp P, Karcher C, Fischer A, *et al.* The ion channel polycystin-2 is required for left-right axis determination in mice. Curr Biol 2002;12:938–943.
13. Allen E, Piontek KB, Garrett-Mayer E, *et al.* Loss of polycystin-1 or polycystin-2 results in dysregulated apolipoprotein expression in murine tissues via alterations in nuclear hormone receptors. Hum Mol Genet 2006;15:11–21.
14. Wu G, D'Agati V, Cai Y, *et al.* Somatic inactivation of Pkd2 results in polycystic kidney disease. Cell 1998;93:177–188.
15. Lu W, Peissel B, Babakhanlou H, *et al.* Perinatal lethality with kidney and pancreas defects, in mice with a targetted pkd1 mutation. Nature Genet 1997;17:179–181.
16. Hassane S, Claij N, Lantinga-van L, *et al.* Pathogenic sequence for dissecting aneurysm formation in a hypomorphic polycystic kidney disease 1 mouse model. Arterioscler Thromb Vasc Biol 2007;27:2177–2183.
17. Lantinga-van Leeuwen IS, Dauwerse JG, Baelde HJ, *et al.* Lowering of Pkd1 expression is sufficient to cause polycystic kidney disease. Hum Mol Genet 2004;13:3069–3077.
18. Sharif-Naeini R, Folgering JHA, Bichet B, *et al.* Polycystin-1 and -2 dosage regulates pressure sensing. Cell 2009;139:587–596.
19. AbouAlaiwi WA, Takahashi M, Mell BR, *et al.* Ciliary polycystin-2 is a mechanosensitive calcium channel involved in nitric oxide signaling cascades. Circ Res 2009;104:860–869.
20. Morel N, Vandenberg G, Ahrabi AK, *et al.* PKD1 haploinsufficiency is associated with altered vascular reactivity and abnormal calcium signaling in the mouse aorta. Pflugers Arch 2009;457:845–856.
21. Kip SN, Hunter LW, Ren Q, *et al.* [Ca2+]i reduction increases cellular proliferation and apoptosis in vascular smooth muscle cells: relevance to the ADPKD phenotype. Circ Res 2005;96:873–880.
22. Lantinga-van Leeuwen IS, Leonhard WN, van der Wal A, *et al.* Kidney-specific inactivation of the Pkd1 gene induces rapid cyst formation in developing kidneys and a slow onset of disease in adult mice. Hum Mol Genet 2007;16:3188–3196.
23. Soriano P. Generalized lacZ expression with the ROSA26 Cre reporter strain. Nat Genet 1999;21:70–71.
24. Bergwerff M, Deruiter MC, Hall S, *et al.* Unique vascular morphology of the fourth aortic arches: possible implications for pathogenesis of type-B aortic arch interruption and anomalous right subclavian artery. Cardiovasc Res 1999;44:185–196.
25. Hierck BP, Iperen LV, GittenbergerdeGroot AC, *et al.* Modified Indirect Immunodetection Allows Study of Murine Tissue with Mouse Monoclonal-Antibodies. J Histochem Cytochem 1994;42:1499–1502.
26. Christensen EI, Nielsen S, Moestrup SK, *et al.* Segmental distribution of the endocytosis receptor gp330 in renal proximal tubules. Eur J Cell Biol 1995;66:349–364.
27. Mulvany MJ, Halpern W. Contractile properties of small arterial resistance vessels in spontaneously hypertensive and normotensive rats. Circ Res 1977;41:19–26.
28. Sequeira Lopez ML, Chernavvsky DR, Nomasa T, *et al.* The embryo makes red blood cell progenitors in every tissue simultaneously with blood vessel morphogenesis. Am J Physiol Regul Integr Comp Physiol 2003;284:R1126–R1137.
29. Wasteson P, Johansson BR, Jukkola T, *et al.* Developmental origin of smooth muscle cells in the descending aorta in mice. Development 2008;135:1823–1832.
30. Sato TN, Qin Y, Kozak CA, *et al.* Tie-1 and tie-2 define another class of putative receptor tyrosine kinase genes expressed in early embryonic vascular system. Proc Natl Acad Sci USA 1993;90:9355–9358.
31. Happe H, Leonhard WN, van der Wal A, *et al.* Toxic tubular injury in kidneys from Pkd1-deletion mice accelerates cystogenesis accompanied by dysregulated planar cell polarity and canonical Wnt signaling pathways. Hum Mol Genet 2009;18:2532–2542.
32. Guyton AC, Coleman TG, Granger HJ. Circulation: overall regulation. Annu Rev Physiol 1972;34:13–46.
33. Fow JE, Averill DB, Barnes KL. Mechanisms of angiotensin-induced hypotension and bradycardia in the medial solitary tract nucleus. Am J Physiol 1994;267(1 Part 2):H259–H266.
34. Montani JP, Van Vliet BN. Understanding the contribution of Guyton's large circulatory model to long-term control of arterial pressure. Exp Physiol 2009;94:382–388.
35. Geng L, Segal Y, Pavlova A, *et al.* Distribution and developmentally regulated expression of murine polycystin. Am J Physiol (Renal physiol) 1997;272:F451–F459.
36. Ong AC, Ward CJ, Butler RJ, *et al.* Coordinate expression of the autosomal dominant polycystic kidney disease proteins, polycystin-2 and polycystin-1, in normal and cystic tissue. Am J Pathol 1999;154:1721–1729.
37. Viana R, Batourina E, Huang H, *et al.* The development of the bladder trigone, the center of the anti-reflux mechanism. Development 2007;134:3763–3769.
38. Michaud J, Russo P, Grignon A, *et al.* Autosomal dominant polycystic kidney disease in the fetus. Am J Med Genet 1994;51:240–246.
39. Verani RR, Silva FG. Histogenesis of the renal cysts in adult (autosomal dominant) polycystic kidney disease: a histochemical study. Mod Pathol 1988;1:457–463.
40. Woolf AS, Price KL, Scambler PJ, *et al.* Evolving concepts in human renal dysplasia. J Am Soc Nephrol 2004;15:998–1007.
41. Gusmano R, Caridi G, Marini M, *et al.* Glomerulocystic kidney disease in a family. Nephrol Dial Transplant 2002;17:813–818.
42. Sharp CK, Bergman SM, Stockwin JM, *et al.* Dominantly transmitted glomerulocystic kidney disease: a distinct genetic entity. J Am Soc Nephrol 1997;8:77–84.
43. Lu W, Shen X, Pavlova A, *et al.* Comparison of Pkd1-targeted mutants reveals that loss of polycystin-1 causes cystogenesis and bone defects. Hum Mol Genet 2001;10:2385–2396.
44. Jiang ST, Chiou YY, Wang E, *et al.* Defining a link with autosomal-dominant polycystic kidney disease in mice with congenitally low expression of Pkd1. Am J Pathol 2006;168:205–220.
45. Abderrahim E, Ben MF, Ben AT, *et al.* Glomerulocystic kidney disease in an adult presenting as end-stage renal failure. Nephrol Dial Transplant 1999;14:1276–1278.
46. Boca M, D'Amato L, Distefano G, *et al.* Polycystin-1 induces cell migration by regulating phosphatidylinositol 3-kinase-dependent cytoskeletal rearrangements and GSK3beta-dependent cell cell mechanical adhesion. Mol Biol Cell 2007;18:4050–4061.
47. Boletta A, Qian F, Onuchic LF, *et al.* Polycystin-1, the gene product of PKD1, induces resistance to apoptosis and spontaneous tubulogenesis in MDCK cells. Mol Cell 2000;6:1267–1273.
48. Appel D, Kershaw DB, Smeets B, *et al.* Recruitment of podocytes from glomerular parietal epithelial cells. J Am Soc Nephrol 2009;20:333–343.